Published in final edited form as:

Glia. 2018 April ; 66(4): 801–812. doi:10.1002/glia.23285.

Glial M6B stabilizes the axonal membrane at peripheral nodes of Ranvier:

Glial M6B preserves the architecture of peripheral nodes of Ranvier

Marie L Bang[1], **Anya Vainshtein**[1], **Hyun-Jeong Yang**[1], **Yael Eshed-Eisenbach**[1], **Jerome Devaux**[2], **Hauke B Werner**[3], and **Elior Peles**[1]

[1]Department of Molecular Cell Biology, Weizmann Institute of Science, Rehovot, Israel

[2]Aix-Marseille University, CNRS, CRN2M-UMR 7286, Marseille, France

[3]Department of Neurogenetics, Max Planck Institute of Experimental Medicine, Goettingen, Germany

Abstract

Glycoprotein M6B and the closely related proteolipid protein (PLP) regulate oligodendrocyte myelination in the central nervous system, but their role in the peripheral nervous system is less clear. Here we report that M6B is located at nodes of Ranvier in peripheral nerves where it stabilizes the nodal axolemma. We show that M6B is co-localized and associates with gliomedin at Schwann cell microvilli that are attached to the nodes. Developmental analysis of sciatic nerves, as well as of myelinating Schwann cells/dorsal root ganglion (DRG) neurons cultures, revealed that M6B is already present at heminodes, which are considered the precursors of mature nodes of Ranvier. However, in contrast to gliomedin, which accumulates at heminodes with or prior to Na^+ channels, we often detected Na^+ channel clusters at heminodes without any associated M6B, indicating that it is not required for initial channel clustering. Consistently, nodal cell adhesion molecules (NF186, NrCAM), ion channels (Nav1.2 and Kv7.2), cytoskeletal proteins (AnkG and βIV spectrin), and microvilli components (pERM, syndecan3, gliomedin), are all present at both heminodes and mature nodes of Ranvier in *Gpm6b* null mice. Using transmission electron microscopy, we show that the absence of M6B results in progressive appearance of nodal protrusions of the nodal axolemma, that are often accompanied by the presence of enlarged mitochondria. Our results reveal that M6B is a Schwann cell microvilli component that preserves the structural integrity of peripheral nodes of Ranvier.

Graphical Abstract

Address correspondence to: Dr. Elior Peles, Department of Molecular Cell Biology, Weizmann Institute of Science, Rehovot, 76100, Israel, peles@weizmann.ac.il.

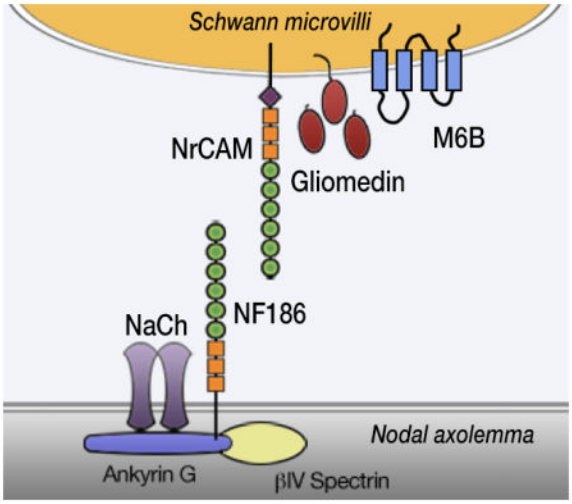

Keywords

PNS; Myelin; Schwann cells Microvilli; Node of Ranvier; M6B proteolipid

INTRODUCTION

The nodes of Ranvier contain a high density of voltage-gated Na^+ channels that drive the propagation of action potentials along the axon. Clustering of these channels on the axolemma is directed by the overlying myelinating oligodendrocyte or Schwann cells through the action of cell adhesion molecules present at both the nodes of Ranvier and the paranodal junctions flanking each node of Ranvier (Eshed-Eisenbach and Peles, 2013; Rasband and Peles, 2015). While nodes in the central nervous system (CNS) are contacted by astrocytes and oligodendrocyte precursor cells, in the peripheral nervous system (PNS), the nodal axolemma is contacted by microvilli emanating from the outer aspect of Schwann cells that myelinate the adjacent internodes.

The initial contact between Schwann cell microvilli processes and the axon during development of myelinated nerves induces the heminodal clustering of Na^+ channels at both sides of the myelin internodes (Vabnick et al., 1996; Ching et al., 1999). Axoglial contact and heminodal channel clustering is mediated by the binding of glial gliomedin and NrCAM to axonal neurofascin 186 (NF186) (Feinberg et al., 2010; Labasque et al., 2011). The latter functions as an attachment site for the scaffolding proteins ankyrin-G (AnkG) and βIV Spectrin, that further recruit Na^+ channels (Rasband and Peles, 2015). Clustering of the nodal complex by gliomedin is enabled by its ability to self-aggregate and bind heparan sulfate proteoglycans (HSPGs) (Eshed et al., 2007; Han and Kursula, 2015). The continuous interaction between gliomedin, NrCAM and NF186 not only mediate the initial clustering of Na^+ channels, but is also required for their long-term maintenance at the nodes of Ranvier (Amor et al., 2014; Desmazieres et al., 2014). Consistent with these observations, autoantibodies to NF186 and gliomedin were reported in patients with multifocal motor neuropathy (MMN), Guillain-Barre syndrome (GBS), and chronic inflammatory

demyelinating polyneuropathy (CIDP) (Stathopoulos et al., 2015; Delmont et al., 2017). Similarly, mutations that impair the ability of gliomedin to bind NF186 results in arthrogryposis multiplex congenita (AMC), a congenital joint contracture caused by decreased fetal movement in utero (Maluenda et al., 2016).

Within the nodal gap, the microvilli are embedded in a dense extracellular matrix (ECM; termed “cementing disc of Ranvier”) enriched in proteoglycans (Melendez-Vasquez et al., 2005; Colombelli et al., 2015). Several cytoplasmic and transmembrane proteins were identified in Schwann cell microvilli: the cytoskeletal ERM proteins (ezrin, radixin, and moesin) (Melendez-Vasquez et al., 2001; Scherer et al., 2001), Rho-A GTPase (Melendez-Vasquez et al., 2004), the 116-kD dystrophin (Dp116) (Occhi et al., 2005), and dystroglycan (α-DG and β-DG) (Saito et al., 2003). The latter recruits perlecan, an HSPG that binds gliomedin and assists in its incorporation into the nodal gap extracellular matrix (ECM) (Colombelli et al., 2015).

Here, we report the identification of membrane glycoprotein M6B (official gene name *Gpm6b*) as a novel component of the nodal Schwann cell microvilli. M6B is a four-transmembrane protein belonging to the proteolipid protein family which mediates intercellular contact, and regulates membrane growth, composition and targeting (Mobius et al., 2008; Fjorback et al., 2009; Werner et al., 2013; Formoso et al., 2016; Patzig et al., 2016; Honda et al., 2017). In the CNS, M6B is expressed by neurons, oligodendrocytes, and astrocytes (Yan et al., 1993; Zhang et al., 2014). M6B has been shown to cooperate with its paralogs proteolipid protein (PLP) and neuronal membrane glycoprotein M6A in regulating membrane growth of oligodendrocytes (Werner et al., 2013) and neurons (Mita et al., 2014), respectively. Outside the nervous system, M6B plays a role in osteoblast differentiation by regulating actin cytoskeleton, ECM remodeling and cell adhesion (Drabek et al., 2011).

MATERIALS AND METHODS

Mice

Mice lacking Gpm6b (M6B^{null}) were previously described (Werner et al., 2013). All experiments were performed in compliance with the relevant laws and institutional guidelines, and were approved by the Weizmann Institute’s Animal Care and Use Committee.

RT-PCR

Total RNA was isolated from mixed DRG cultures, DRG neurons, or Schwann cells using TRI-reagent (Sigma). Sciatic nerve RNA was obtained from freshly dissected P1-P7 wild type rat sciatic nerves. cDNA was synthesized using SuperScript II (Invitrogen). PCR amplification of M6B and gliomedin was done using the following primers: gliomedin, GGGAGCAGCGCGAGGACAG and CTTGGTCACCTTTGGCACCTG; M6B ACACCAGTGACCATGCCTTTCC and GACATCCACACAGATCTGCTCCA; actin GAGCACCCTGTGCTGCTCACCGAGG and GTGGTGGTGAAGCTGTAGCCACGCT.

Antibodies

The following antibodies were used: Rabbit antibodies to gliomedin (720) (Eshed et al., 2007), M6B (8547) (Werner et al., 2013), βIV Spectrin (C9831) (Yang et al., 2004), NF186 (MNF2) (Tait et al., 2000); Rat antibody to Caspr (h190CT) (Feinberg et al., 2010); mouse antibodies to gliomedin (94) (Eshed et al., 2005) and Caspr (275) (Poliak et al., 1999). Anti-Syndecan 3 (ab63932), anti-NrCAM (ab24344), and anti-β-catenin (ab22656) were purchased from abcam, anti-Pan Na^+ channel (K58/35) and anti-ezrin (3c12) from Sigma Aldrich, anti-Ankyrin G (N106/65) and anti-Necl4 (N244/5) from NeuroMab, anti-pERM (3141) from Cell Signaling Technology, anti-Nav1.6 (ASC_009) from Alomone Lab, and anti-Pan neurofascin (AF3235) from R&D systems.

Tissue culture methods

Dissociated spinal cord cells were prepared from mice embryos at day 13.5 of gestation as described previously (Golan et al., 2008). Cells were grown for two weeks in medium (DMEM with 4.5 mg/mL glucose, 10 ng/mL biotin, 50 nM hydrocortisone, 5 μg/ml apotransferrin, 100 μM putrescine, 20 nM progesterone, 30 nM selenium) containing 10 μg/ml insulin, and then for 2–3 weeks in the absence of insulin to induce myelination. Dissociated dorsal root ganglia (DRG) myelinating cultures were prepared as described previously (Eshed et al., 2005; Amor et al., 2017). Cultures of purified mouse DRG neurons were prepared by growing dissociated DRGs in medium supplemented with 10μM uridine/ 10μM 5′-Fluoro 2′-deoxyuridine (FuDR; Sigma) to eliminate fibroblasts and Schwann cells as described previously (Eshed et al., 2005). Cultures of rat Schwann cells grown alone or with purified mouse DRG neurons were prepared as described previously (Feinberg et al., 2010). For clustering experiments, COS7 transfected with expression plasmids containing mouse M6B (splice isoform αβTMDω) (Werner et al., 2013), or Necl4-myc/his (Spiegel et al., 2007) either alone or with gliomedin. Media containing 0.5–1μg/ml of the NF186Fc or human Fc together with Cy3-conjugated anti–human-Fc antibody (Jackson Laboratories), were incubated with the transfected cells for 30 min at room temperature. Unbound proteins were removed by three washes with PBS and the cells were fixed with 4% paraformaldehyde (PFA) and used for immunolabeling (see below). Production of Fc fusion proteins containing the extracellular domain of gliomedin (Gliomedin-Fc; residues 49–543), its collagen like domain (COL-Fc; residues 49–294), or the olfactomedin domain (OLF-Fc; residues 288–543) was done as described previously (Eshed et al., 2007).

Pulldown and Western blot analysis

For pull-down experiments, HEK293 expressing M6B were lysed using a buffer containing 50 mM Tris, pH 7.5, 150 mM NaCl, 1 mM EGTA, 10% glycerol, and 1% Triton X-100 (Tx100), supplemented with a protease inhibitors mixture (Sigma-Aldrich). Cleared lysates were incubated with Fc-fusion proteins bound to protein Sepharose-A beads for 12hrs at 4°C. Beads were subsequently washed twice with ice cold PBS containing 0.1% Tx100 and once with PBS. Proteins were eluted from the beads using SDS sample buffer in 40°C for 1hr. Samples were resolved by SDS-PAGE on 12% polyacrylamide SDS gels and transferred to a PVDF membrane. Western blot analysis was performed as described previously (Amor et al., 2014).

Immunofluorescence and electron microscopy

Teased sciatic nerves and frozen optic nerve sections were prepared as described previously (Amor et al., 2017). Slides (either tissues or cultured cells) were post fixed with cold methanol, washed with PBS and incubated with blocking solution (5% fish skin gelatin or normal goat serum and 0.1% Triton X-100, in PBS) for 1 hour at room temperature. Samples were incubated at 4°C with the mixture of primary antibodies diluted in blocking solution for 12 hours, washed with PBS, incubated for 45 minutes at ambient temperature with fluorophore-coupled secondary antibodies (Jackson Laboratories and Molecular Probes), and then washed with PBS and mounted with Elvanol. Fluorescence images were obtained either using Nikon eclipse E1000 microscope with a Hamamatsu ORCA-ER CCD camera, or using a Zeiss LSM700 confocal microscope. Images were acquired and processed using the Zen2012 software (Carl Zeiss). For electron microscopy, sciatic nerves were exposed and fixed with 4% PFA, 2.5% glutaraldehyde, and 0.1M sodium cacodylate pH 7.4 in PBS for 40 minutes. Nerves were then removed and incubated over-night in the same fixative. Samples processing was carried out as previously described (Novak et al., 2011). Sections were imaged using a Philips CM-12 transmission electron microscope.

Experimental design and statistical analysis

M6B-positive NaCh clusters in P2, P5 and P7 sciatic nerve were quantified from confocal microscope images. A total of 423, 560 and 329 nodes from P2, P5 and P7, respectively, were counted (3 mice per age). Quantification of nodal protrusion was carried out using longitudinal electron microscopy images in a double-blinded manner by two separate persons. Total of 90 mutant and 60 wild type nodes were analyzed at P15, and 81 mutant and 59 wild type nodes were analyzed at P75. The percent of nodal protrusions was calculated from the average percentage of three P15 or six P75 animals from each genotype. Statistical significance was determined using the student's two-tailed t-test.

RESULTS

Glycoprotein M6B is present at PNS nodes of Ranvier

We have recently identified M6B in a screen for proteins that are present in non-myelinated neuronal membrane domains (Redmond et al., 2016). To examine the localization of M6B in peripheral nerve, we double-labeled teased rat sciatic nerve using antibodies to M6B and myelin-associated glycoprotein (MAG; to mark non-compact myelin), gliomedin (to mark the glial aspect of the nodes), Caspr (to mark the paranodal junction), or to Na^+ channels (to mark the nodal axolemma) (Figure 1A–D). In these nerves, M6B immunoreactivity was concentrated and colocalized with gliomedin at the nodes of Ranvier. Labeling of pulled nerve preparations using antibodies to Na^+ channels and M6B revealed that M6B is present at the glial, but not the axonal aspect of the nodes (Figure 1E). In contrast to rat tissue, M6B immunoreactivity in teased mouse sciatic nerve was detected in both the nodes of Ranvier and sometimes at the paranodal Schwann cell loops (Figure 1F–G). However, the latter was still present in nerves isolated from mice lacking M6B, indicating that it should be considered as a non-specific background of the antibody (Figure 1H).

To examine whether M6B is also present at nodes in the CNS, we co-labeled cryosections of spinal cord containing the attached spinal roots using antibodies to M6B, gliomedin and pan-neurofascin (the latter labels both nodes and paranodal junction) (Figure 2A). Immunolabeling of gliomedin was used to distinguish PNS from CNS tissue, since gliomedin is only present at PNS nodes (Eshed et al., 2005). M6B co-localized with gliomedin at nodes of Ranvier in the spinal nerve roots but was detected neither in the spinal cord (Figure 2A) nor in the optic nerve (Figure 2B). Similarly, nodal M6B immunoreactivity was detected in myelinated cultures prepared from dorsal root ganglia (DRG), but not from spinal cord (Figure 2C–D). These results demonstrate that while in the CNS M6B is part of the compact myelin (Werner et al., 2013), in peripheral nerves it is a major component of the nodes of Ranvier.

M6B is a Schwann cell component of the node

To determine the cellular origin of M6B in PNS nodes, we immunolabeled cultured Schwann cells using antibodies to M6B and β-catenin (Figure 3A) or ezrin (Figure 3B–C). M6B was enriched in β-catenin-labeled membrane protrusions that often bridge two adjacent Schwann cells. M6B was present along the entire length of these cellular protrusions including their distal tip, an area that extended beyond the proximal part that contained ezrin (Figure 3C). RT-PCR analysis revealed that M6B transcript is expressed by cultured Schwann cells, but not by DRG neurons (Figure 3D). To further examine whether the nodal M6B is of Schwann cell origin, we prepared myelinating cultures using different combinations of DRG neuron and Schwann cells isolated from wild type and *Gpm6b* null mice (Figure 3E). M6B was present at the nodes of Ranvier in cultures containing *Gpm6b* null neurons and wild type Schwann cells, similarly to the ones composed of both wild type neurons and Schwann cells. Altogether, these findings suggest that M6B is a glial component of the PNS nodes.

M6B appears at heminodes during development

The assembly of PNS nodes involves initial clustering of the nodal complex at heminodes followed by a convergence of two heminodes and the formation of mature nodes (Feinberg et al., 2010). In myelinating cultures M6B was present at both heminodes and mature nodes that were flanked by two Caspr-labeled paranodes (Figure 4A). To better understand the role of M6B in peripheral nerves, we examined its expression and distribution during the development of peripheral nerves. M6B transcript was detected in the sciatic nerve by RT-PCR already at P1 before nodes are formed, and continued to be expressed after mature nodes are formed at P7 (data not shown). However, immunolabeling of sciatic nerves using antibodies to M6B and Na^+ channels revealed that while M6B is present in the majority (95%) of nodes at P7, only 59% and 71% of the nodal clusters contained M6B at P2 and P5 respectively (Figure 4B–C). These results demonstrate that while M6B could be detected at heminodes, it appears after the initial nodal complex has been assembled.

Nodes of Ranvier are assembled in the absence of M6B

The late appearance of M6B at nodes suggests that it may not be required for the initial clustering of the nodal complex. To examine whether this is the case, as well as whether M6B is required to maintain nodal clusters once they are formed, we examine the

distribution of various nodal components in sciatic nerves of *Gpm6b*$^{-/-}$ mice (Werner et al., 2013). As depicted in Figure 5A, the localization of nodal transmembrane proteins (NF186, NrCAM, and Nav1.6), intracellular cytoskeletal adapter proteins (Ankyrin G and bIV Spectrin), or glial proteins (phosphorylated ERM and gliomedin) was similar to wild type nerves. Furthermore, we did not register any significant difference in the nodal gap length between *Gpm6b*$^{-/-}$ and wild type mice (Data not shown). Since node formation depends on both heminodal clustering and paranodal restriction mechanisms (Feinberg et al., 2010; Labasque et al., 2011), the apparent normal nodes observed in sciatic nerves from *Gpm6b*$^{-/-}$ mice could eventually form in spite of a potential abnormal clustering of heminodes similar to what was observed after genetic deletion of gliomedin, NrCAM (Feinberg et al., 2010), or b-DG (Colombelli et al., 2015). To examine this possibility, we made use of myelinating cultures, which allow better analysis of the early steps in node formation. Immunolabeling of mixed myelinating cultures of embryonic DRGs isolated from *Gpm6b*$^{-/-}$ and wild type mice revealed that all the examined components (i.e., NF186, NrCAM, NaCh, AnkG, bIV Spectrin, pERM, and gliomedin) were present at heminodes in both genotypes (Figure 5B). These results indicate that M6B is not essential for the clustering of Na^+ channels at the nodes of Ranvier.

M6B interacts with gliomedin

The nodal axonal complex containing ion channels and cell adhesion molecules interacts with a network of transmembrane glial proteins and ECM components that is thought to stabilize it and ensure saltatory conduction (Eshed-Eisenbach and Peles, 2013; Rasband and Peles, 2015). Given the precise co-localization of M6B and gliomedin, we set out to investigate whether they physically interact. A soluble protein containing the extracellular domain (ECD) of gliomedin fused to human Fc, but not the Fc alone pulled down M6B from transfected HEK-293 cells (Figure 6A–B). To further map the protein module in gliomedin that interacts with M6B, we used Fc-fusion proteins containing its olfactomedin domain (OLF), which binds NF186 and NrCAM (Eshed et al., 2005; Eshed et al., 2007; Labasque et al., 2011), or its collagen-like domain (COL) which mediates its interaction with Schwann cell ECM (Eshed et al., 2005; Eshed et al., 2007; Labasque et al., 2011). M6B was pulled down with gliomedin ECD and OLF domains, but not with the COL domain (Figure 6C–D), indicating that gliomedin interacts with M6B through its olfactomedin domain. Interestingly, the soluble extracellular domain of gliomedin did not bind to cells expressing M6B (data not shown), suggesting that the interaction between these two proteins occurs when both are present on the same membrane (i.e., in cis). In accordance, a soluble Fc-fusion protein containing the extracellular domain of NF186 (NF186-Fc) clustered M6B, but not Necl4 in COS7 cells co-expressing gliomedin (Figure 6E–F). In contrast, M6B was not co-clustered upon aggregation of Necl4 with a soluble Necl1-Fc (Figure 6G). NF186-Fc did not bind M6B expressing cells (data not shown), indicating that clustering of M6B (Figure 6E) is mediated by its binding to gliomedin. Taken together, these results suggest that M6B interacts with gliomedin at the microvilli, and that the M6B/gliomedin complex further contributes to the formation of the multi-protein nodal network by binding both glial NrCAM and axonal NF186.

M6B KO mice exhibit an increased number of nodal protrusions

The localization of M6B in Schwann cell microvilli has prompted us to examine the morphology of the nodes of Ranvier in *Gpm6b*$^{-/-}$ mice by transmission electron microscopy. Longitudinal (Figure 7A, C) and cross (Figure 7B, D) sections of sciatic nerve revealed that the nodal axolemma was contacted by Schwann cell microvilli in both genotypes. However, compared to wild type nerves, *Gpm6b*$^{-/-}$ nodes exhibited a significant frequency of axonal protrusions that often contained vesicles and enlarged mitochondria (Figure 7C–D). These nodal protrusions were of different widths, ranging from wide membrane bulges that encompassed the entire nodal gap (Figure 7G–H) to thin finger-like protrusions (Figure 7I–J). The number of nodes showing membrane abnormalities in *Gpm6b*$^{-/-}$ mice range from 30%–40% compared to 10% abnormalities that were observed in wild type mice (Figure 7E–F). There was no statistically-significant increase in the number of nodal protrusion detected with age. The pronounced expansion of the nodal axolemma in *Gpm6b*$^{-/-}$ mice suggests that the presence of M6B at the Schwann cell microvilli preserves the structural integrity of peripheral nodes of Ranvier.

DISCUSSION

The nodes of Ranvier in peripheral nerves are contacted by microvilli arising from the outer collar of the Schwann cells that myelinate the flanking internodes (Hildebrand, 1971; Ichimura and Ellisman, 1991). These microvilli develop from early glial processes that contacts the nodal axolemma, and hence were suggested to mediate axon-glia interactions necessary for the clustering of Na^+ channels and the assembly of the nodes of Ranvier (Melendez-Vasquez et al., 2001). In agreement, disruption of Schwann cell microvilli impairs heminodal clustering of these channels (Feinberg et al., 2010; Colombelli et al., 2015). In addition to their role in the initial clustering of Na^+ channels, a continuous axoglial interaction mediated by binding of microvillar gliomedin and glial NrCAM to axonal NF186 is required for the long-term maintenance of these channels at the nodes of Ranvier (Amor et al., 2014).

In the present study, we have identified glycoprotein M6B as a Schwann cell microvilli component of peripheral nodes of Ranvier. This conclusion is based on the following observations: ***i.*** co-localization of M6B with microvilli proteins such as gliomedin at both heminodes and mature nodes, ***ii.*** the presence of M6B immunoreactivity in the glial aspect of pulled sciatic nerve preparation, ***iii.*** its localization at ERM-positive membrane processes and cell-cell contacts in cultured Schwann cells, ***iv.*** the respective presence and absence of M6B transcript in isolated Schwann cells and sensory neurons, and ***v.*** the appearance of M6B at the nodes of Ranvier in cultures consisting of wild type Schwann cells and *Gpm6b*$^{-/-}$ neurons. M6B was detected at nodes in sciatic nerve, as well as in sections of dorsal and ventral roots (data not shown), demonstrating that it is present at nodes of Ranvier in both sensory and motor nerves. In contrast, M6B was completely absent from the nodes in the CNS (i.e., optic nerve and spinal cord). While M6B is a constituent of compact myelin in the CNS (Werner et al., 2013), in the PNS it is present in the Schwann cell microvilli, which represent a unique compartment that is devoid of the proteins of compact myelin. This may suggest the existence of mechanism that sort M6B to the microvilli similar to other

microvilli components such as ERM and syndecan. Notably, such a mechanism is likely distinct from the one employed by gliomedin, which requires the nodal adhesion molecules NF186 and NrCAM (Feinberg et al., 2010). In accordance, we found that M6B is still present at the nodal microvilli in sciatic nerve of mice lacking gliomedin or NrCAM (data not shown). The identification of M6B as a nodal component may also be of clinical significance given the presence of autoantibodies to nodal and paranodal proteins in Guillain-Barre syndrome and chronic inflammatory demyelinating polyneuropathy (Stathopoulos et al., 2015). One hypothesis based on our results is that autoantibodies to M6B may cause an increase in the nodal axolemma surface and a slower nerve conduction (Arancibia-Carcamo et al., 2017; Delmont et al., 2017).

Previous observations in both peripheral and central nodes demonstrated the existence of compensatory and functionally overlapping nodal gap components (Feinberg et al., 2010; Susuki et al., 2013; Colombelli et al., 2015). At the nodal gap, M6B localizes with several cell adhesion molecules, proteoglycans and ECM components. These proteins are engaged in multiple interactions that regulate the formation and maintenance of the nodes of Ranvier (Feinberg et al., 2010; Colombelli et al., 2015). M6B is a novel part of this interaction network by binding the olfactomedin domain of gliomedin, which also mediates the interaction of the latter with both NF186 and NrCAM (Eshed et al., 2005). Interestingly, disruptive mutations in this domain results in Arthrogryposis multiplex congenita in humans (Maluenda et al., 2016). Furthermore, M6B may serve as a link between a microvilli adhesion complex that consists of gliomedin, NrCAM, dystroglycan and perlecan to the cytoskeleton by binding to ERM proteins (Coffey et al., 2009) that are present in the Schwann cell microvilli (Melendez-Vasquez et al., 2001; Scherer et al., 2001). Our data suggest that the interaction between M6B and gliomedin occurs in a *cis* manner, i.e., with both proteins present on the same membrane. This is reminiscent of the mode of interaction between gliomedin and NrCAM on the Schwann cell microvillar membrane (Feinberg et al., 2010). However, while the expression of NrCAM at the Schwann cell microvilli is a prerequisite for the accumulation of gliomedin (Feinberg et al., 2010), the interaction between M6B and gliomedin is not necessary for the localization of the latter at the axoglial interface. This conclusion is also supported by the observation that M6B appeared at heminodes after gliomedin and Na^+ channels. Similarly, and in contrast to gliomedin, which is required for the clustering of Na^+ channels (Feinberg et al., 2010; Amor et al., 2014), M6B is neither necessary for the initial clustering of these channels at heminodes nor for their presence at mature nodes of Ranvier.

Although M6B does not play a predominant role in the assembly of the axonodal complex (i.e., NF186, AnkG, bIV spectrin and Na^+ channels), it is critical for preserving the morphological integrity of the nodal axolemma. Electron microscopy analysis of longitudinal sections of sciatic nerves of mice lacking M6B revealed that 30–40% of the nodes exhibit membrane protrusions, which varied in shape and size. These were not distributed symmetrically on the axonal circumference and were often detected only on one side of the axon perimeter. Our results suggest that the presence of M6B at the Schwann cell microvilli is required for the maintenance of the nodal axolemma. Variation in nodal surface area could result in increased nodal capacitance and the intracellular axial resistance, which are expected to result in reduced conduction speed (Arancibia-Carcamo et al., 2017).

However, despite the morphological abnormality detected, sciatic nerves isolated from mice lacking M6B showed no significant changes in conduction velocity, amplitude, duration, and refractory period (data not shown). The lack of changes in nerve conduction in these animals may be due to the fact that a large number of nodes appeared normal (60%), as well as the observation that the nodal protrusions often did not encompass the entire axolemma. In this regard, it should also be noted that although pronounced nodal abnormalities were detected by EM, no increase in the length of the nodes was detected by immunofluorescence microscopy. Interestingly, nodal protrusions without an overall change in the length of the nodes were also found in sciatic nerves of mice lacking dystroglycan, another constituent of the microvilli adhesion complex which indirectly associates with gliomedin through perlecan (Colombelli et al., 2015).

How does the presence of M6B on the Schwann cell microvilli affect the structure of the underlying axonal membrane? Tetraspanin proteins are involved in the formation of various tubular cell membrane structures including microvilli (Singethan and Schneider-Schaulies, 2008; Bari et al., 2011). They regulate cell morphogenesis by altering the membrane curvature, as well as by mediating membrane-dependent cytoskeletal reorganization. Despite the absence of sequence homology between members of the proteolipid family (i.e., PLP, M6A and M6B) and the tetraspanin family, the structural similarity is striking, in particular when considering the tetraspanin subgroup with two disulfide bridges in the second extracellular loop (Fuchsova et al., 2009). One of the most distinctive functional features of proteolopids and tetraspanins is their ability to interact with multiple proteins and to form lateral associations with each other, as well as with other transmembrane proteins including cell adhesion molecules, growth factors, and integrins (Gudz et al., 2002; Hemler, 2005). The latter is of particular interest as tetraspanins were shown to regulate integrin-mediated adhesion strengthening, a process whereby cells become increasingly resistant to detachment after binding a ligand. Furthermore, M6B could also regulate the formation of membrane complexes by controlling cellular trafficking as recently suggested for the serotonin transporter, SERT (Fjorback et al., 2009). Hence, one possibility to consider is the involvement of M6B in generation of a cell surface complex mediating Schwann cell-axon signaling that controls membrane structure in axons. Such a signaling mechanism is likely to affect the underlying submembrane axonal cytoskeleton at the nodes. This idea is supported by the observations showing that mutations in spectrins results in the formation of membrane protrusions similar to those we detected here after the depletion of M6B (Lacas-Gervais et al., 2004; Yang et al., 2004). The possibility that M6B in the glia may affect cytoskeletal organization within the axon is intriguing and will be the topic of future research.

Acknowledgments

We thank Matt Rasband and Peter Brophy for antibodies. This work was supported by the NIH (R01NS097428), the Israel Science Foundation, and the Dr. Miriam and Sheldon G. Adelson Medical Research Foundation E.P. is the Incumbent of the Hanna Hertz Professorial Chair for Multiple Sclerosis and Neuroscience.

References

Amor V, Feinberg K, Eshed-Eisenbach Y, Vainshtein A, Frechter S, Grumet M, Rosenbluth J, Peles E. Long-term maintenance of Na^+ channels at nodes of Ranvier depends on glial contact mediated by gliomedin and NrCAM. J Neurosci. 2014; 34:5089–5098. [PubMed: 24719088]

Amor V, Zhang C, Zhang O, Zollinger DR, Eshed-Eisenbach Y, Brophy PJ, Rasband MN, Peles E. The paranodal cytoskeleton clusters Na+ channels at nodes of Ranvier. eLife. 2017; 6:e21391.

Arancibia-Carcamo IL, Ford MC, Cossell L, Ishida K, Tohyama K, Attwell D. Node of Ranvier length as a potential regulator of myelinated axon conduction speed. Elife. 2017:6.

Bari R, Guo Q, Xia B, Zhang YH, Giesert EE, Levy S, Zheng JJ, Zhang XA. Tetraspanins regulate the protrusive activities of cell membrane. Biochemical and biophysical research communications. 2011; 415:619–626. [PubMed: 22079629]

Ching W, Zanazzi G, Levinson SR, Salzer JL. Clustering of neuronal sodium channels requires contact with myelinating Schwann cells. J Neurocytol. 1999; 28:295–301. [PubMed: 10739572]

Coffey GP, Rajapaksa R, Liu R, Sharpe O, Kuo CC, Krauss SW, Sagi Y, Davis RE, Staudt LM, Sharman JP, Robinson WH, Levy S. Engagement of CD81 induces ezrin tyrosine phosphorylation and its cellular redistribution with filamentous actin. J Cell Sci. 2009; 122:3137–3144. [PubMed: 19654214]

Colombelli C, Palmisano M, Eshed-Eisenbach Y, Zambroni D, Pavoni E, Ferri C, Saccucci S, Nicole S, Soininen R, McKee KK, Yurchenco PD, Peles E, Wrabetz L, Feltri ML. Perlecan is recruited by dystroglycan to nodes of Ranvier and binds the clustering molecule gliomedin. J Cell Biol. 2015; 208:313–329. [PubMed: 25646087]

Delmont E, Manso C, Querol L, Cortese A, Berardinelli A, Lozza A, Belghazi M, Malissart P, Labauge P, Taieb G, Yuki N, Illa I, Attarian S, Devaux JJ. Autoantibodies to nodal isoforms of neurofascin in chronic inflammatory demyelinating polyneuropathy. Brain. 2017; 140:1851–1858. [PubMed: 28575198]

Desmazieres A, Zonta B, Zhang A, Wu LM, Sherman DL, Brophy PJ. Differential stability of PNS and CNS nodal complexes when neuronal neurofascin is lost. J Neurosci. 2014; 34:5083–5088. [PubMed: 24719087]

Drabek K, van de Peppel J, Eijken M, van Leeuwen JP. GPM6B regulates osteoblast function and induction of mineralization by controlling cytoskeleton and matrix vesicle release. J Bone Miner Res. 2011; 26:2045–2051. [PubMed: 21638316]

Eshed Y, Feinberg K, Carey DJ, Peles E. Secreted gliomedin is a perinodal matrix component of peripheral nerves. J Cell Biol. 2007; 177:551–562. [PubMed: 17485493]

Eshed Y, Feinberg K, Poliak S, Sabanay H, Sarig-Nadir O, Spiegel I, Bermingham JR Jr, Peles E. Gliomedin mediates Schwann cell-axon interaction and the molecular assembly of the nodes of Ranvier. Neuron. 2005; 47:215–229. [PubMed: 16039564]

Eshed-Eisenbach Y, Peles E. The making of a node: a co-production of neurons and glia. Current opinion in neurobiology. 2013; 23:1049–1056. [PubMed: 23831261]

Feinberg K, Eshed-Eisenbach Y, Frechter S, Amor V, Salomon D, Sabanay H, Dupree JL, Grumet M, Brophy PJ, Shrager P, Peles E. A glial signal consisting of gliomedin and NrCAM clusters axonal Na+ channels during the formation of nodes of Ranvier. Neuron. 2010; 65:490–502. [PubMed: 20188654]

Fjorback AW, Muller HK, Wiborg O. Membrane glycoprotein M6B interacts with the human serotonin transporter. J Mol Neurosci. 2009; 37:191–200. [PubMed: 18581270]

Formoso K, Garcia MD, Frasch AC, Scorticati C. Evidence for a role of glycoprotein M6a in dendritic spine formation and synaptogenesis. Molecular and cellular neurosciences. 2016; 77:95–104. [PubMed: 27793698]

Fuchsova B, Fernandez ME, Alfonso J, Frasch AC. Cysteine Residues in the Large Extracellular Loop (EC2) Are Essential for the Function of the Stress-regulated Glycoprotein M6a. Journal of Biological Chemistry. 2009; 284:32075–32088. [PubMed: 19737934]

Golan N, Adamsky K, Kartvelishvily E, Brockschnieder D, Mobius W, Spiegel I, Roth AD, Thomson CE, Rechavi G, Peles E. Identification of Tmem10/Opalin as an oligodendrocyte enriched gene

using expression profiling combined with genetic cell ablation. Glia. 2008; 56:1176–1186. [PubMed: 18571792]

Gudz TI, Schneider TE, Haas TA, Macklin WB. Myelin proteolipid protein forms a complex with integrins and may participate in integrin receptor signaling in oligodendrocytes. J Neurosci. 2002; 22:7398–7407. [PubMed: 12196561]

Han H, Kursula P. The olfactomedin domain from gliomedin is a beta-propeller with unique structural properties. J Biol Chem. 2015; 290:3612–3621. [PubMed: 25525261]

Hemler ME. Tetraspanin functions and associated microdomains. Nat Rev Mol Cell Bio. 2005; 6:801–811. [PubMed: 16314869]

Hildebrand C. Ultrastructural and light-microscopic studies of the developing feline spinal cord white matter. I. The nodes of Ranvier. Acta Physiol Scand Suppl. 1971; 364:81–109. [PubMed: 4109396]

Honda A, Ito Y, Takahashi-Niki K, Matsushita N, Nozumi M, Tabata H, Takeuchi K, Igarashi M. Extracellular Signals induce Glycoprotein M6a Clustering of Lipid-rafts and associated Signaling Molecules. J Neurosci. 2017; 37:4046–4064. [PubMed: 28275160]

Ichimura T, Ellisman MH. Three-dimensional fine structure of cytoskeletal-membrane interactions at nodes of Ranvier. J Neurocytol. 1991; 20:667–681. [PubMed: 1719139]

Labasque M, Devaux JJ, Leveque C, Faivre-Sarrailh C. Fibronectin type III-like domains of neurofascin-186 protein mediate gliomedin binding and its clustering at the developing nodes of Ranvier. J Biol Chem. 2011; 286:42426–42434. [PubMed: 22009740]

Lacas-Gervais S, Guo J, Strenzke N, Scarfone E, Kolpe M, Jahkel M, De Camilli P, Moser T, Rasband MN, Solimena M. BetaIVSigma1 spectrin stabilizes the nodes of Ranvier and axon initial segments. J Cell Biol. 2004; 166:983–990. [PubMed: 15381686]

Maluenda J, Manso C, Quevarec L, Vivanti A, Marguet F, Gonzales M, Guimiot F, Petit F, Toutain A, Whalen S, Grigorescu R, Coeslier AD, Gut M, Gut I, Laquerriere A, Devaux J, Melki J. Mutations in GLDN, Encoding Gliomedin, a Critical Component of the Nodes of Ranvier, Are Responsible for Lethal Arthrogryposis. Am J Hum Genet. 2016; 99:928–933. [PubMed: 27616481]

Melendez-Vasquez C, Carey DJ, Zanazzi G, Reizes O, Maurel P, Salzer JL. Differential expression of proteoglycans at central and peripheral nodes of Ranvier. Glia. 2005; 52:301–308. [PubMed: 16035076]

Melendez-Vasquez CV, Einheber S, Salzer JL. Rho kinase regulates schwann cell myelination and formation of associated axonal domains. J Neurosci. 2004; 24:3953–3963. [PubMed: 15102911]

Melendez-Vasquez CV, Rios JC, Zanazzi G, Lambert S, Bretscher A, Salzer JL. Nodes of Ranvier form in association with ezrin-radixin-moesin (ERM)-positive Schwann cell processes. Proc Natl Acad Sci U S A. 2001; 98:1235–1240. [PubMed: 11158623]

Mita S, de Monasterio-Schrader P, Funfschilling U, Kawasaki T, Mizuno H, Iwasato T, Nave KA, Werner HB, Hirata T. Transcallosal Projections Require Glycoprotein M6-Dependent Neurite Growth and Guidance. Cereb Cortex. 2014; 25:4111–4125. [PubMed: 24917275]

Mobius W, Patzig J, Nave KA, Werner HB. Phylogeny of proteolipid proteins: divergence, constraints, and the evolution of novel functions in myelination and neuroprotection. Neuron Glia Biol. 2008; 4:111–127. [PubMed: 19497142]

Novak N, Bar V, Sabanay H, Frechter S, Jaegle M, Snapper SB, Meijer D, Peles E. N-WASP is required for membrane wrapping and myelination by Schwann cells. J Cell Biol. 2011; 192:243–250. [PubMed: 21263026]

Occhi S, Zambroni D, Del Carro U, Amadio S, Sirkowski EE, Scherer SS, Campbell KP, Moore SA, Chen ZL, Strickland S, Di Muzio A, Uncini A, Wrabetz L, Feltri ML. Both laminin and Schwann cell dystroglycan are necessary for proper clustering of sodium channels at nodes of Ranvier. J Neurosci. 2005; 25:9418–9427. [PubMed: 16221851]

Patzig J, Kusch K, Fledrich R, Eichel MA, Luders KA, Mobius W, Sereda MW, Nave KA, Martini R, Werner HB. Proteolipid protein modulates preservation of peripheral axons and premature death when myelin protein zero is lacking. Glia. 2016; 64:155–174. [PubMed: 26393339]

Poliak S, Gollan L, Martinez R, Custer A, Einheber S, Salzer JL, Trimmer JS, Shrager P, Peles E. Caspr2, a new member of the neurexin superfamily, is localized at the juxtaparanodes of

myelinated axons and associates with K+ channels. Neuron. 1999; 24:1037–1047. [PubMed: 10624965]

Rasband MN, Peles E. The Nodes of Ranvier: Molecular Assembly and Maintenance. Cold Spring Harb Perspect Biol. 2015; 8:a020495. [PubMed: 26354894]

Redmond SA, Mei F, Eshed-Eisenbach Y, Osso LA, Leshkowitz D, Shen YA, Kay JN, Aurrand-Lions M, Lyons DA, Peles E, Chan JR. Somatodendritic Expression of JAM2 Inhibits Oligodendrocyte Myelination. Neuron. 2016; 91:824–836. [PubMed: 27499083]

Saito F, Moore SA, Barresi R, Henry MD, Messing A, Ross-Barta SE, Cohn RD, Williamson RA, Sluka KA, Sherman DL, Brophy PJ, Schmelzer JD, Low PA, Wrabetz L, Feltri ML, Campbell KP. Unique role of dystroglycan in peripheral nerve myelination, nodal structure, and sodium channel stabilization. Neuron. 2003; 38:747–758. [PubMed: 12797959]

Scherer SS, Xu T, Crino P, Arroyo EJ, Gutmann DH. Ezrin, radixin, and moesin are components of Schwann cell microvilli. Journal of neuroscience research. 2001; 65:150–164. [PubMed: 11438984]

Singethan K, Schneider-Schaulies J. Tetraspanins: Small transmembrane proteins with big impact on membrane microdomain structures. Communicative & integrative biology. 2008; 1:11–13. [PubMed: 19704780]

Spiegel I, Adamsky K, Eshed Y, Milo R, Sabanay H, Sarig-Nadir O, Horresh I, Scherer SS, Rasband MN, Peles E. A central role for Necl4 (SynCAM4) in Schwann cell-axon interaction and myelination. Nature neuroscience. 2007; 10:861–869. [PubMed: 17558405]

Stathopoulos P, Alexopoulos H, Dalakas MC. Autoimmune antigenic targets at the node of Ranvier in demyelinating disorders. Nat Rev Neurol. 2015; 11:143–156. [PubMed: 25623793]

Susuki K, Chang KJ, Zollinger DR, Liu Y, Ogawa Y, Eshed-Eisenbach Y, Dours-Zimmermann MT, Oses-Prieto JA, Burlingame AL, Seidenbecher CI, Zimmermann DR, Oohashi T, Peles E, Rasband MN. Three mechanisms assemble central nervous system nodes of Ranvier. Neuron. 2013; 78:469–482. [PubMed: 23664614]

Tait S, Gunn-Moore F, Collinson JM, Huang J, Lubetzki C, Pedraza L, Sherman DL, Colman DR, Brophy PJ. An oligodendrocyte cell adhesion molecule at the site of assembly of the paranodal axo-glial junction. J Cell Biol. 2000; 150:657–666. [PubMed: 10931875]

Vabnick I, Novakovic SD, Levinson SR, Schachner M, Shrager P. The clustering of axonal sodium channels during development of the peripheral nervous system. J Neurosci. 1996; 16:4914–4922. [PubMed: 8756423]

Werner HB, Kramer-Albers EM, Strenzke N, Saher G, Tenzer S, Ohno-Iwashita Y, De Monasterio-Schrader P, Mobius W, Moser T, Griffiths IR, Nave KA. A critical role for the cholesterol-associated proteolipids PLP and M6B in myelination of the central nervous system. Glia. 2013; 61:567–586. [PubMed: 23322581]

Yan Y, Lagenaur C, Narayanan V. Molecular cloning of M6: identification of a PLP/DM20 gene family. Neuron. 1993; 11:423–431. [PubMed: 8398137]

Yang Y, Lacas-Gervais S, Morest DK, Solimena M, Rasband MN. BetaIV spectrins are essential for membrane stability and the molecular organization of nodes of Ranvier. J Neurosci. 2004; 24:7230–7240. [PubMed: 15317849]

Zhang Y, Chen K, Sloan SA, Bennett ML, Scholze AR, O'Keeffe S, Phatnani HP, Guarnieri P, Caneda C, Ruderisch N, Deng S, Liddelow SA, Zhang C, Daneman R, Maniatis T, Barres BA, Wu JQ. An RNA-sequencing transcriptome and splicing database of glia, neurons, and vascular cells of the cerebral cortex. J Neurosci. 2014; 34:11929–11947. [PubMed: 25186741]

Main Points

- M6B as a new glial component of the nodes of Ranvier
- M6B is co-localized and associates with gliomedin at Schwann cell microvilli
- Absence of M6B leads to morphological abnormalities of the nodal axolemma

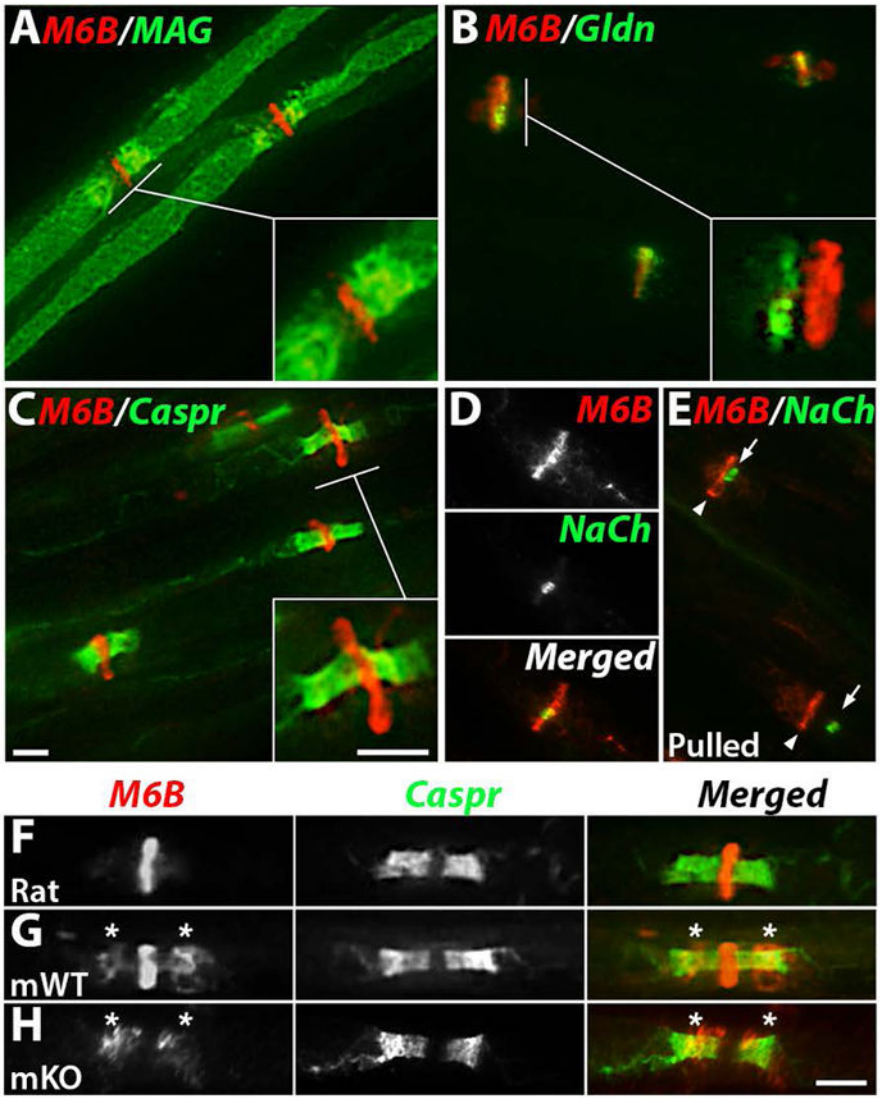

Figure 1. M6B is localized at the nodes of Ranvier

A–C. Teased rat sciatic nerves immunolabeled with antibodies to M6B and myelin associated glycoprotein (MAG) (A), gliomedin (Gldn) (B), and Caspr (C). Insets show magnification of the indicated node in each panel. **D–E.** Teased rat sciatic nerves immunolabeled with antibodies to M6B and Na^+ channels (NaCh). The single and merged channels are shown in D. Pulling of the nerves during teasing (E) results in separation between the NaCh-labeled nodal axolemma (arrows) and the glial microvilli (arrowhead). **F–H.** Teased sciatic nerves isolated from adult rat (F), wild type mice (mWT) (G), or mice lacking Gpm6b (mKO) (H) immunolabeled with antibodies to M6B and Caspr. Asterisks mark non-specific immunoreactivity of M6B at the paranodes. Scale bars: 5 μm.

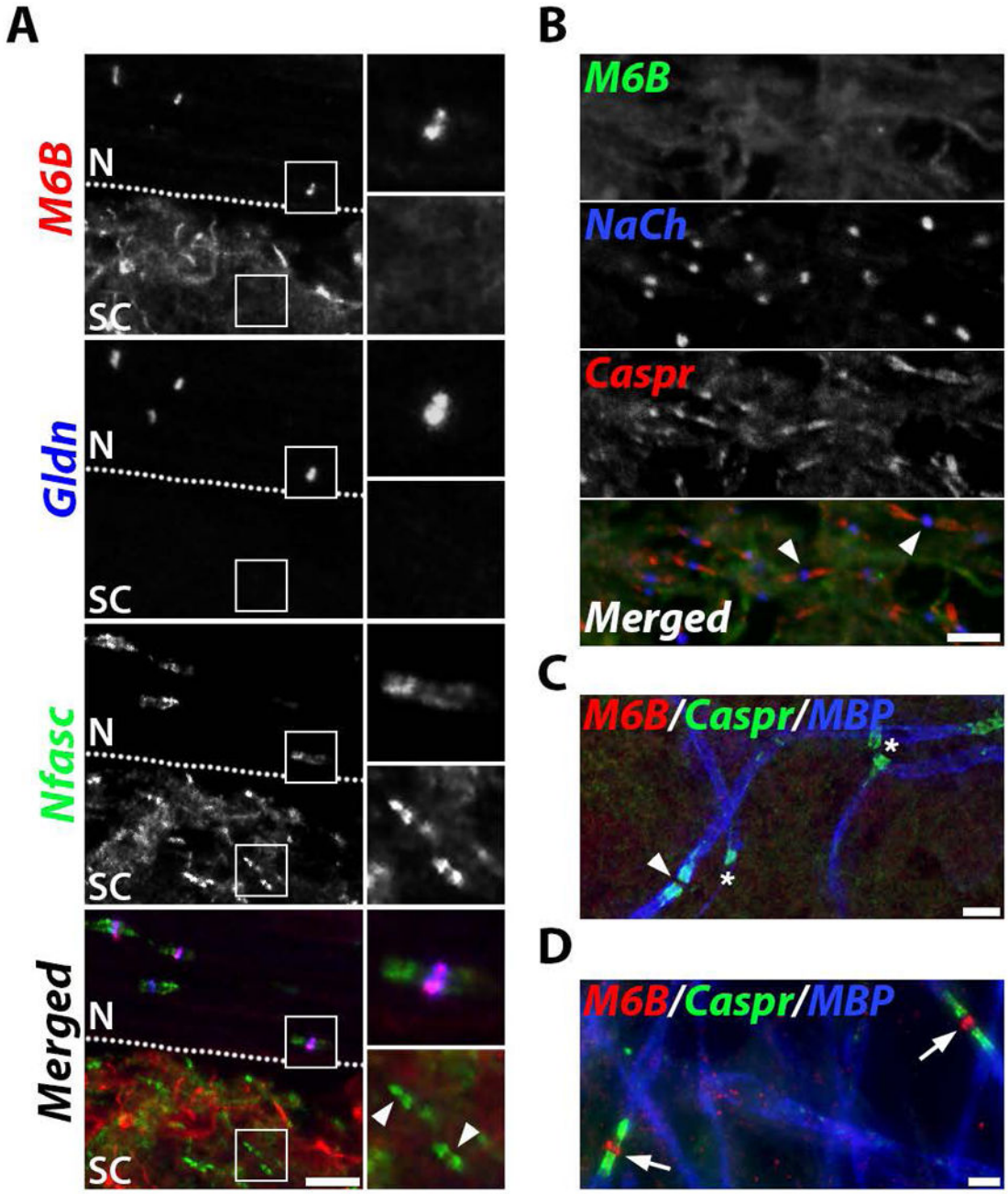

Figure 2. M6B is specific to PNS nodes

A. Sections of rat spinal cord with attached nerve roots were immunolabeled with antibodies to M6B, gliomedin (Gldn) and pan-Neurofascin (Nfasc). A stippled line marks the boundary between the nerve root (N) and the spinal cord (SC). Higher magnification of the boxed areas is shown on the right of each panel. Arrowheads mark the location of the nodes. **B.** Optic nerve sections immunolabeled with antibodies to M6B, Na^+ channels (NaCh), and Caspr. The nodes are marked by arrowheads. **C**–**D.** Myelinating mouse spinal cord (C) and mixed DRG cultures (D) immunolabeled with antibodies to M6B, Caspr and myelin basic protein (MBP). M6B is absent from nodes (arrowheads) and heminodes (asterisks) in CNS

cultures, but is present at the nodes (arrows) in PNS cultures. Scale bars: A, 10 μm; B–D, 5 μm.

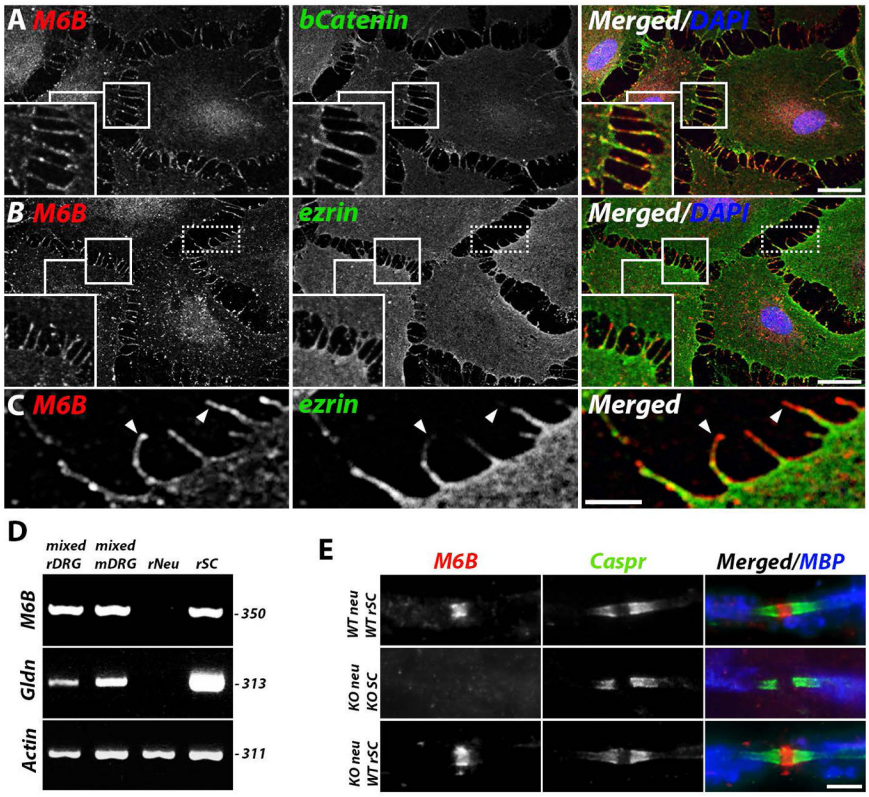

Figure 3. M6B is a glial component of the node

A–C. M6B is present in Schwann cell protrusions. Cultures of rat Schwann cells labeled with antibodies to M6B and β-catenin (A), or ezrin (B–C). Schwann cells nuclei are labeled with Dapi. Higher magnifications of the boxed areas are shown in the inset in each panel. **C.** Higher magnification of the dotted area in B. Arrowheads mark the presence of M6B at the edge of ezrin-labeled cell processes. **B.** RT-PCR analysis of mRNA isolated from mixed rat (rDRG) or mouse (mDRG) DRG cultures, isolated rat DRG neurons (rNeu) or Schwann cells (rSC) using primers for M6B, gliomedin (Gldn) or actin. The location of size markers (in bp) is shown on the right. **C.** Myelinating cultures prepared from wild type DRG neurons (*WTneu*) and rat Schwann cells (*WTrSC*) (upper panels), *Gpm6b* null DRG neurons (*KOneu*) and *Gpm6b* null Schwann cells (*KOSC*) (middle panels), or *Gpm6b* null DRG neurons (*KOneu*) and wild type rat Schwann cells (*WTrSC*). Cultures were immunolabeled with antibodies to M6B, Caspr and MBP. Scale bars: A–B, 10 μm; C, 5 μm.

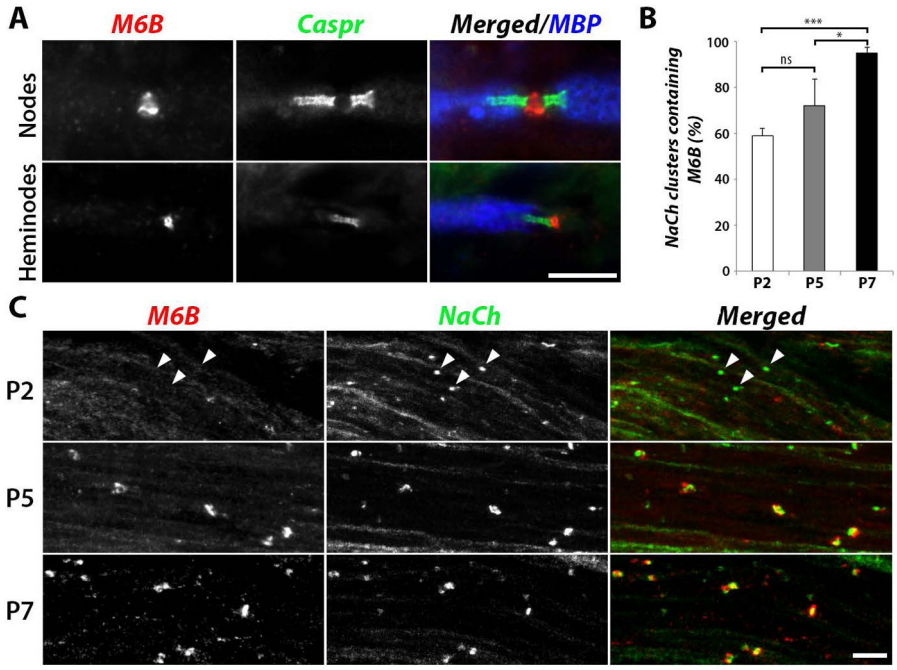

Figure 4. M6B is present at developing nodes

A. Images of myelinated mouse DRG neurons/Schwann cell cultures immunolabeled with antibodies to M6B, Caspr and MBP. M6B is present at both mature nodes (upper panels), as well as at heminodes (bottom panels). **B–C.** Immunofluorescence labeling (C) and quantification (B) of 2-, 5-, and 7-day-old rat sciatic nerve with antibodies to M6B and Na^+ channels (NaCh). Arrowheads mark the location of Na^+ channels-containing nodes lacking M6B. The number of Na^+ channels clusters containing M6B increased with age (P2=423, P5=560, P7=329 nodes from three animals; *p≤0.05, ***p≤ 0.0001). Error bars indicate standard error of mean (SEM). Scale bars: 10 μm.

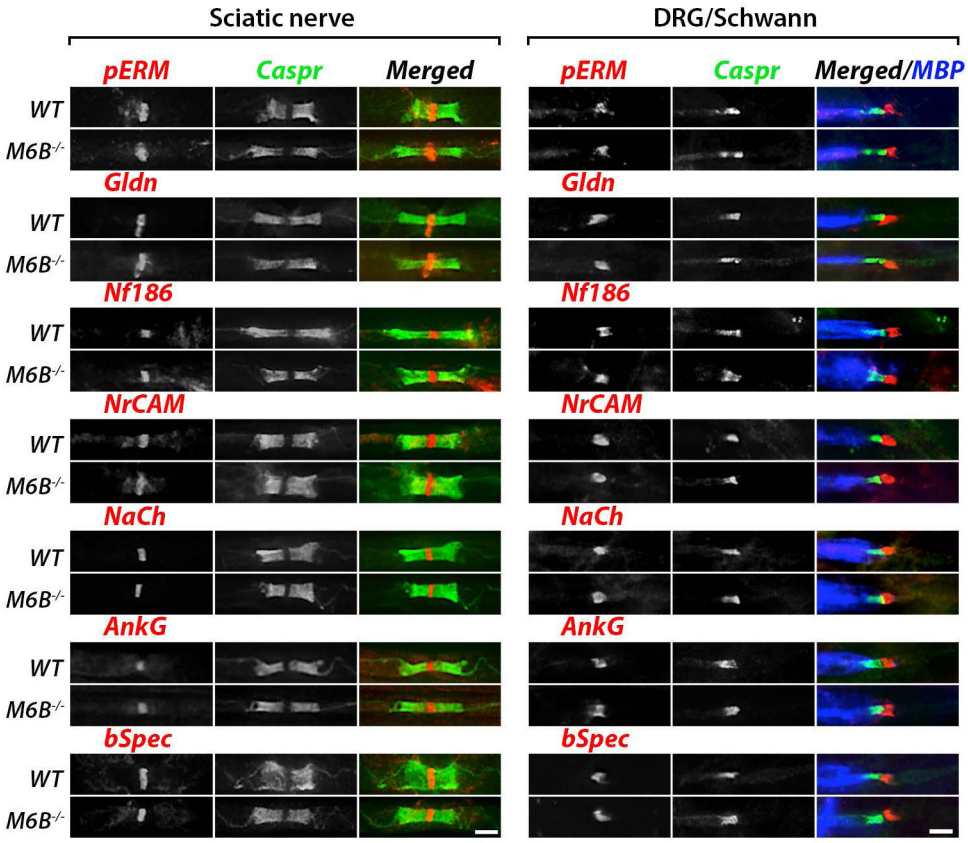

Figure 5. Nodes of Ranvier and heminodes are formed in the absence of M6B

Teased sciatic nerves (left panels) or mixed myelinated DRG cultures (right panels) prepared from wild type (*WT*) or *Gpm6b* null (*M6B*$^{-/-}$) mice were immunolabeled using antibodies to Caspr (to mark the paranodes), MBP (to mark compact myelin), and to various nodal proteins as indicated; phosphorylated ERM (pERM), gliomedin (Gldn), neurofascin 186 (NF186), NrCAM, Na^+ channels (NaCh), ankyrin-G (AnkG), and βIV-Spectrin (bSpec). Scale bars: 5μm.

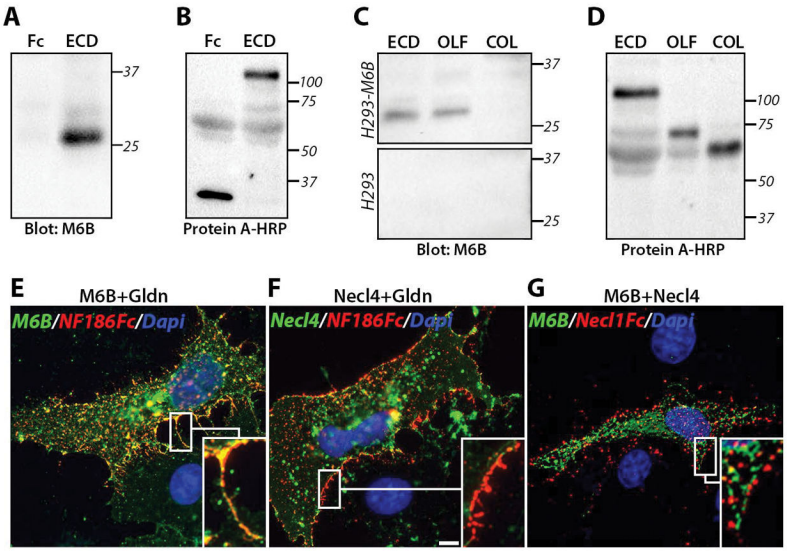

Figure 6. M6B interacts with gliomedin

A. Pulldown of M6B by the extracellular domain of gliomedin. Lysates of HEK-293 cells expressing M6B were incubated with a fusion protein containing the extracellular domain of gliomedin fused to human Fc (ECD), or the Fc protein alone (Fc). Bound proteins were resolved by SDS-gel and subjected to Western blot analysis using an antibody to M6B. **B.** Western blot analysis using protein A-HRP showing the presence of the Fc-fusion proteins used for pulldown. **C.** A similar pulldown experiment using Fc-fusion proteins containing the entire extracellular domain of gliomedin (ECD), its olfactomedin domain (OLF), or its amino terminal region containing the coiled-coil and the collagen domains (COL). **D.** Western blot analysis using protein A-HRP showing the presence of the Fc-fusion proteins used for pulldown. **E–G.** Clustering of gliomedin by NF186-Fc induces aggregation of M6B. COS7 cells expressing gliomedin and M6B (E), gliomedin and Necl-4 (F), or M6B and Necl4 (G) were incubated with Cy3-coupled NF186-Fc (E-F) or Necl1-Fc (G) before fixation and immunolabeling with antibodies to M6B or Necl4 as indicated. Dapi was used to label the nuclei. Note that gliomedin clustering by NF186-Fc induced co-clustering of M6B but not of Necl4. Higher magnifications of the boxed areas are shown in the inset in each panel. Scale bar: 10 μm.

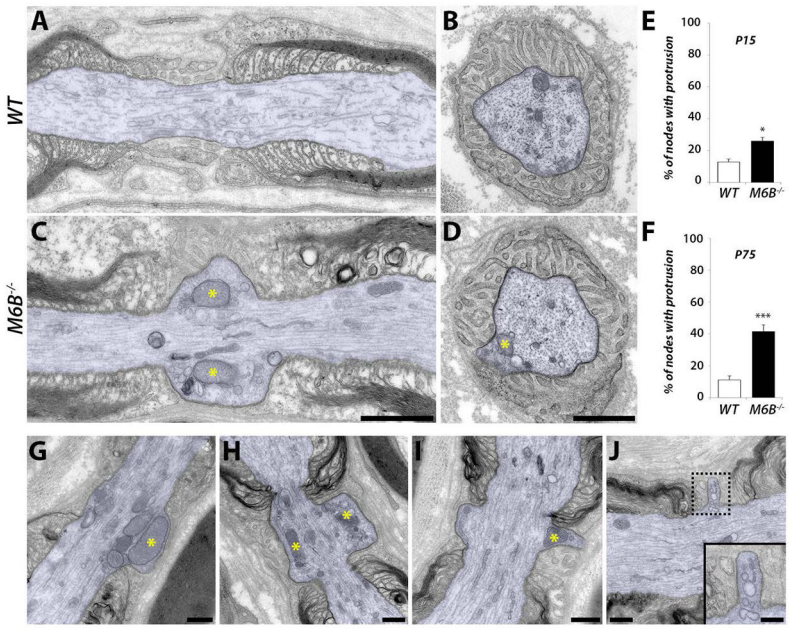

Figure 7. Absence of M6B results in abnormal nodal morphology

A–D. EM images of longitudinal (A, C) and cross-sections (B, D) of sciatic nerves of 2.5-month-old wild type (*WT*; A–B) and *Gpm6b* null ($M6B^{-/-}$) showing nodes of Ranvier. **E–F.** The number of nodal protrusions was significantly higher in *Gpm6b* null ($M6B^{-/-}$) than in wild type (*WT*) at P15 (E) and P75 (F) (E: *WT*=90 nodes, $M6B^{-/-}$=60 nodes from three mice of each genotype; F: *WT*=59 nodes, $M6B^{-/-}$=81 nodes from six mice of each genotype; *p≤0.05, ***p≤ 0.0001). Error bars indicate standard error of mean (SEM). Using two-way ANOVA, revealed that the increase in nodal protrusion with age is not statistical significant. **G–J.** Additional images showing nodal protrusions observed in sciatic nerves of $M6B^{-/-}$ mice. Inset in J shows a higher magnification of the dotted box. The presence of mitochondria is marked by asterisks. Scale bars: A–D, 1 μm; G–J, 0.5 μm; J inset, 0.25 μm.